Full Paper

Propellants, Explosives, Pyrotechnics

DOI: 10.1002/prep.201800237

Thermal Behavior and Detonation Characterization of 3,3-Dinitroazetidinium Salicylate

Biao Yan,*[a, b, c] Hongya Li,[b] Haixia Ma,*[c] Fengqi Zhao,*[a] Yajun Ma,[b] Zhifang Zhang,[b] Ya Zhang,[b] and Zhiyong Zhang[d]

Abstract: The thermal behavior of 3,3-dinitroazetidinium salicylate (DNAZ·SA) was studied under a non-isothermal condition by DSC and TG/DTG methods. The intense exothermic decomposition processes of DSC curves were analyzed to obtain its kinetic parameters. The self-accelerating decomposition temperature (T_{SADT}), thermal ignition temperature (T_{TIT}), and critical temperatures of thermal explosion (T_b) were obtained to evaluate its thermal stability and safety. The DFT was used to calculate its band structure; the energy gap was obtained to evaluate its impact insensitivity. Its detonation velocity (*D*) and detonation pressure (*P*) were estimated using the nitrogen equivalent equation according to the experimental density. The above results of DNAZ·SA were compared with those of 3,3-dinitroazetidinium 3,5-dinitrosalicylate (DNAZ·DNS), and the effect of nitro group on them were discussed, which results indicate that the nitro group increases the safety and energy simultaneously.

Keywords: 3,3-Dinitroazetidinium salicylate (DNAZ·SA) · Thermal safety · Detonation characteristic · DFT

1 Introduction

Energetic materials (EMs) are widely used in military affairs, construction business, mining, tunnel engineering, civil fireworks and firecrackers, and so on. Safety and energy are the two most important concerns for EMs. Four-membered ring is a strained ring, it makes a compound with strain energy. The dinitro- and trinitro-derivatives of azetidine contain the strained ring system (Theoretical calculation results show that the strain energy of 1,3,3-trinitroazetidine (TNAZ) is 152.7 kJ mol^{-1} [1]), and this structural feature makes them good candidates for EMs. Initial reports of TNAZ and 3,3-dinitroazetidine (DNAZ) were concentrated on their synthesis [2–4]. As a weak alkali, DNAZ can react with salicylic acid producing solid energetic salt 3,3-dinitroazetidinium salicylate (DNAZ·SA, Figure 1). However, there is no literature has reported on the safety and energy of DNAZ·SA by now. In order to deepen the study of structure-activity relationship, the thermal stability and safety of DNAZ·SA were compared with 3,3-dinitroazetidinium 3,5-dinitrosalicylate (DNAZ·DNS, Figure 1) through the thermal behavior and the thermal safety temperature. Their impact insensitivities were compared through the energy gap. The detonation characterization for DNAZ·SA was also performed and compared with that of DNAZ·DNS.

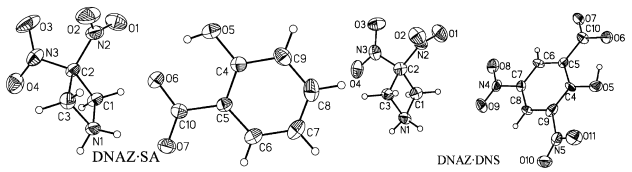

Figure 1. Molecular structures of DNAZ·SA and DNAZ·DNS.

2 Experimental Section

2.1 Materials

The DNAZ·SA was synthesized and purified according to a reported method [5]. A colorless single crystal of DNAZ·SA (CCDC 751995) [5] was obtained. The mass fraction purity of

[a] *B. Yan, F. Zhao*
Science and Technology on Combustion and Explosion Laboratory
Xi'an Modern Chemistry Research Institute
Xi'an 710065, P. R. China
**e-mail: yanbiaoly@foxmail.com*
zhaofqi@163.com
[b] *B. Yan, H. Li, Y. Ma, Z. Zhang, Y. Zhang*
School of Chemistry and Chemical Engineering
Yulin University
Yulin 719000, P. R. China
[c] *B. Yan, H. Ma*
School of Chemical Engineering
Northwest University
Xi'an 710069, P. R. China
**e-mail: yanbiaoly@foxmail.com*
mahx@nwu.edu.cn
[d] *Z. Zhang*
School of Information Science and Technology
Northwest University
Xi'an 710127, P. R. China

Supporting information for this article is available on the WWW under https://doi.org/10.1002/prep.201800237

the crystal of DNAZ·SA was measured by high performance liquid chromatography (HPLC type shimadzu LC-10AT, infusion pump type LC-10ATvp, detector type SPD-10Avp, the mobile phase is absolute ethyl alcohol) and found to be above 0.998.

2.2 Thermal Decomposition Conditions

The TG/DTG and DSC analysis of DNAZ·SA was conducted using a Q600SDT (TA, USA) instrument under a nitrogen atmosphere (purity, 99.999%) at a flow rate of 100 mL min^{-1} with the sample mass of about 0.823 mg, and the heating rates were 2.5, 5.0, 10.0, and 15.0 °C min^{-1}. The temperature and heat were calibrated using pure indium (purity, 99.99%) and tin (purity, 99.99%) particles by onset temperatures under a nitrogen atmosphere at the same conditions.

2.3 Quantum Chemical Calculations

The calculations in this study were performed using the CASTEP code [6] based on density functional theory (DFT). The ultrasoft pseudopotentials [7] were employed to describe the coulomb interactions between the valence electrons and pseudo-ion core. The electronic wave functions were obtained by a density-mixing scheme [8] and the structures were relaxed by using the Broyden, Fletcher, Goldfarb, and Shannon (BFGS) methods [9]. The local density approximation (LDA) functional was employed, it was proposed by Ceperley and Alder [10] and parameterized by Perdew and Zunger [11] named CA-PZ. Brillouin zone sampling was performed by using the Monkhost-Pack [12] scheme with a *k*-point grid of $1 \times 2 \times 1$. The cutoff energy of plane waves was 380.0 eV. The values of the kinetic energy cutoff and the *k*-point grid were determined to ensure the convergence of total energies. Starting from the single crystal structural data of DNAZ·SA [5] and DNAZ·DNS [13], the geometry relaxation was performed to allow the ionic configurations, cell shape, and volume to change. The compressibility was set as soft. In the geometry relaxation, the total energy of the system was converged less than 5.0×10^{-6} eVatom^{-1}, the residual force was less than 0.1 eVnm^{-1}, the displacement of atoms was less than 5.0×10^{-3} nm, and the residual bulk stress was less than 0.02 GPa.

3 Results and Discussion

3.1 Thermal Behavior

Typical DSC and TG/DTG curves for DNAZ·SA at heating rate of 10.0 °C min^{-1} are shown in Figures 2 and 3. The DSC curve indicates that the thermal behavior of DNAZ·SA can be divided into two stages. The first stage is a melting process (67.71 Jg^{-1}), the extrapolated onset temperature (T_e, melting point) and peak temperature (T_p) are 106.15 °C and 115.84 °C, respectively. The TG curves show that this stage with a mass loss of 0.30%. There is no melting process for DNAZ·DNS [13], it shows that the lattice energy of DNAZ·DNS is higher than that of DNAZ·SA, and the molecular structure analysis for DNAZ·SA and DNAZ·DNS indicates that the nitro group increases the lattice energy. The second stage is an intense exothermic decomposition process (−1381 Jg^{-1}), the T_e and T_p are 141.18 °C and 153.30 °C, respectively, they are all lower than those of DNAZ·DNS (158.83 °C and 161.78 °C) [13], which indicates that DNAZ·DNS has better thermal stability than DNAZ·SA, and the molecular structure analysis for DNAZ·SA and DNAZ·DNS indicates that the nitro group improves the thermal stability. The TG curves show that this stage with a mass loss of 55.64%. The temperature data on DSC of its intense exothermic decomposition process are listed in Table 1.

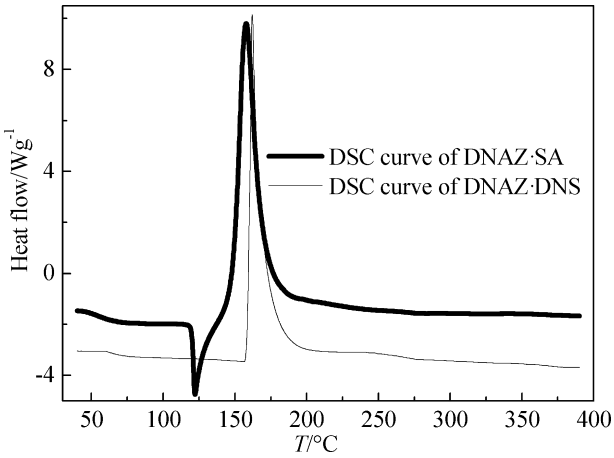

Figure 2. DSC curves of DNAZ·SA and DNAZ·DNS [13] at a heating rate of 10.0 °C min^{-1}.

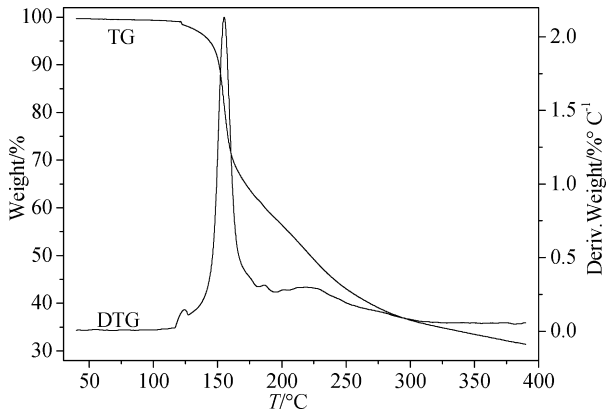

Figure 3. TG/DTG curve of DNAZ·SA at a heating rate of 10.0 °C min^{-1}.

Table 1. The values of T_e, T_p, and ΔH_d of the intense exothermic decomposition process for DNAZ·SA determined from the DSC curves at various heating rates (β).

β/°C min^{-1}	T_e/°C	T_p/°C	ΔH_d/Jg^{-1}
2.5	122.62	130.69	−1381
5.0	132.19	141.90	
10.0	141.18	153.30	
15.0	144.31	158.05	

3.2 Non-isothermal Reaction Kinetics

To explore the reaction mechanism of the intense exothermic decomposition process of DNAZ·SA and obtain the corresponding kinetic parameters [apparent activation energy (E_a) and pre-exponential constant (A)] and the most probable kinetic model functions [$G(\alpha)$ and $f(\alpha)$]. The DSC curves at the heating rates of 2.5, 5.0, 10.0 and 15.0 °C min^{-1} were dealt with the mathematic means, and the temperature data corresponding to the conversion degrees (α) were found. Six integral methods (MacCallum-Tanner, Šatava-Šesták, Agrawal, General integral, Universal integral, and Flynn-Wall-Ozawa) and one differential method (Kissinger) were employed [14–22]. The values of E_a were obtained by Flynn-Wall-Ozawa's method from the iso-conversional DSC curves at the heating rates of 2.5, 5.0, 10.0 and 15.0 °C min^{-1}, and the E_a-α relation is shown in Figure 4. One can see that the E_a has slight change in the range of 0.05–0.625 (α), and this range was selected to calculate the non-isothermal reaction kinetics.

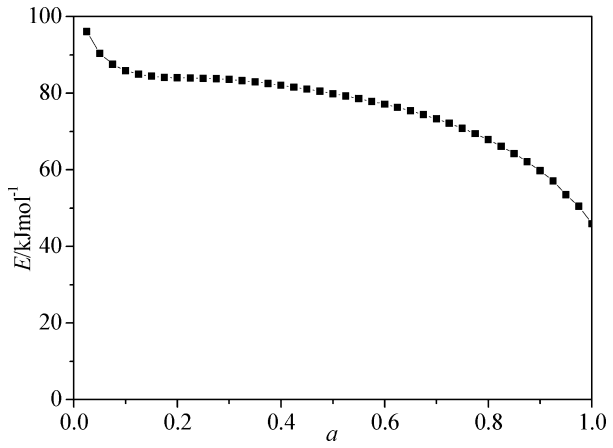

Figure 4. E_a vs α curve of DNAZ·SA by Flynn-Wall-Ozawa's method.

Forty-one types of kinetic model functions and the original data were put into the five integral equations (MacCallum-Tanner, Šatava-Šesták, Agrawal, general integral, and universal integral) to calculate the parameters. The E_a, A, linear correlation coefficient (r), standard mean square deviation (Q), and believable factor (d, where $d=(1-r)Q$) are presented in Table 2. The values of E_a and lg$A$ obtained from a single non-isothermal DSC curve are in good agreement with the calculated values obtained by the methods of Kissinger and Flynn-Wall-Ozawa. Therefore, we conclude that the reaction mechanism of the intense exothermic decomposition process for DNAZ·SA is classified as Mampel power law $G(\alpha)=\alpha^{1/2}$ and $f(\alpha)=2\alpha^{1/2}$. Substituting $f(\alpha)=2\alpha^{1/2}$, $E_a=$ 92.61 kJ mol^{-1}, and $A=10^{9.07}$ s^{-1} into Equation (1),

$$\frac{d\alpha}{dT}=\frac{A}{\beta}f(\alpha)e^{-E_a/RT} \quad (1)$$

Where β is heating rate (°C min^{-1}), R is gas constant (8.314 J mol^{-1}K^{-1}), and T is temperature (K).

The kinetic equation of the intense exothermic decomposition reaction for DNAZ·SA can be described as $d\alpha/dT=2\alpha^{1/2}(10^{9.07}/\beta)\exp(-1.1138\times10^4/T)$.

The E_a and A of the intense exothermic decomposition reaction for DNAZ·SA are 92.61 kJ mol^{-1} and $10^{9.07}$ s^{-1}, respectively, they are all lower than those of DNAZ·DNS (130.83 kJ mol^{-1} and $10^{13.80}$ s^{-1}) [13], which indicates that DNAZ·DNS has better thermal stability than DNAZ·SA.

3.3 Thermal Safety Studies

The values (T_{e0} and T_{p0}) of the T_e and T_p of DNAZ·SA corresponding to $\beta\rightarrow0$ are obtained from Equation (2) [23–24], and the self-accelerating decomposition temperature (T_{SADT}) of DNAZ·SA is obtained from Equation (3) [25]. The values are listed in Table 3.

$$T_{e(or\ p)}=T_{e0(or\ p0)}+a\beta+b\beta^2+c\beta^3 \quad (2)$$

Where a, b and c are equation coefficients.

$$T_{SADT}=T_{e0} \quad (3)$$

The thermal ignition temperature (T_{be0} or T_{TIT}) of DNAZ·SA is obtained by substituting E_{eO} and T_{e0} into Equation (4) [25], and the critical temperature of thermal explosion (T_{bp0} or T_b) of DNAZ·SA is obtained by substituting E_{pO} and T_{p0} into Equation (4) [23]. The values are listed in Table 3.

$$T_{be0(orbp0)}=\frac{E_{eO(orpO)}-\sqrt{E^2_{eO(orpO)}-4E_{eO(orpO)}RT_{e0(orp0)}}}{2R} \quad (4)$$

From Table 3, one can find that the T_{SADT}, T_{p0}, T_{TIT} and T_b of DNAZ·DNS are higher than those of DNAZ·SA, so it is easy to conclude that the nitro group improves the thermal stability and safety.

Table 2. Kinetic parameters for the intense exothermic decomposition process of DNAZ·SA.

Method	β/°C min^{-1}	E_a/kJ mol^{-1}	lg(A/s^{-1})	r	Q	d
MacCallum-Tanner	2.5	111.01	11.73	0.9960	4.20×10^{-3}	1.69×10^{-5}
	5	88.98	8.75	0.9993	7.00×10^{-4}	4.68×10^{-7}
	10	82.04	7.82	0.9977	2.42×10^{-3}	5.59×10^{-6}
	15	86.05	8.34	0.9900	1.04×10^{-2}	1.04×10^{-4}
Šatava-Šesták	2.5	112.99	12.03	0.9960	4.20×10^{-3}	1.69×10^{-5}
	5	92.19	9.22	0.9993	7.00×10^{-4}	4.68×10^{-7}
	10	85.64	8.35	0.9977	2.42×10^{-3}	5.59×10^{-6}
	15	89.43	8.84	0.9900	1.04×10^{-2}	1.04×10^{-4}
Agrawal	2.5	112.18	11.93	0.9954	2.24×10^{-2}	1.01×10^{-4}
	5	90.14	8.93	0.9992	3.77×10^{-3}	2.97×10^{-6}
	10	83.05	7.97	0.9972	1.30×10^{-2}	3.58×10^{-5}
	15	86.92	8.48	0.9882	5.57×10^{-2}	6.56×10^{-4}
General integral	2.5	112.18	11.93	0.9954	2.24×10^{-2}	1.01×10^{-4}
	5	90.14	8.93	0.9992	3.77×10^{-3}	2.97×10^{-6}
	10	83.05	7.97	0.9972	1.30×10^{-2}	3.58×10^{-5}
	15	86.92	8.48	0.9882	5.57×10^{-2}	6.56×10^{-4}
Universal integral	2.5	108.30	10.37	0.9952	2.20×10^{-2}	1.05×10^{-4}
	5	86.72	7.51	0.9992	3.61×10^{-3}	2.94×10^{-6}
	10	80.10	6.64	0.9971	1.26×10^{-2}	3.63×10^{-5}
	15	84.21	7.17	0.9876	5.49×10^{-2}	6.78×10^{-4}
Mean		92.61	9.07			
Flynn-Wall-Ozawa	E_{eO}[a]	104.96		0.9949	3.54×10^{-3}	
	E_{pO}[b]	88.47		0.9978	1.57×10^{-3}	
Kissinger	E_K[c]	86.10	8.55	0.9974	8.18×10^{-3}	
Mean(E_{eO},E_{pO}, E_K)		93.18				

[a]E_{eO} is the E_a obtained from the T_e by Flynn-Wall-Ozawa's method. [b]E_{pO} is the E_a obtained from the T_p by Flynn-Wall-Ozawa's method. [c]E_K is the E_a obtained from the T_p by Kissinger's method.

Table 3. The derivative parameters for DNAZ·SA and DNAZ·DNS.

Compound	T_{SADT}/°C	T_{p0}/°C	T_{TIT}/°C	T_b/°C
DNAZ·SA	108.13	114.20	120.40	129.43
DNAZ·DNS	133.04[13]	135.61[13]	145.00[13]	147.55[13]

3.4 Band Structure

The band structures of DNAZ·SA and DNAZ·DNS are shown in Figures S1–S2. The origin of the energy is taken to be the Fermi level. Clearly, the structures are similar and they appear to vary only in the width of the energy band and the flatness of the top of the valence band. Band gap is an important parameter to characterize the electronic structure of solids. The energy gaps of DNAZ·SA and DNAZ·DNS between valence and conduction bands are 1.150 eV and 2.114 eV, respectively. When the molecular structure is similar, the smaller the band gap, the easier the electron transfers from the valence band to the conduction band, and the more the solid becomes decomposed and exploded [26, 27]. It may be thus inferred that the impact insensitivity for the two crystals increases in the following sequence: DNAZ·SA < DNAZ·DNS, and the molecular structure analysis for DNAZ·SA and DNAZ·DNS shows that the nitro group increases the impact insensitivity.

3.5 Detonation Characterization

Detonation velocity (D) and detonation pressure (P) are the most important detonation characterization for EMs. The values of D and P of an explosive can be predicted from the nitrogen equivalent equation (NE equation) shown as Equations (5)–(7) [28].

$$\sum N = 100\sum x_i N_i / M \tag{5}$$

$$D = (690 + 1160\rho_0)\ \sum N \tag{6}$$

$$P = 1.092(\rho_0 \sum N)^2 - 0.574 \tag{7}$$

Where ΣN is the nitrogen equivalent of detonation products, x_i is the mole number of certain detonation product produced by one mole of explosive, N_i is the nitrogen equivalent index of a certain detonation product, M is the molecular mass of an explosive, and ρ_0 is the density of an explosive (g cm^{-3}).

The nitrogen equivalent indexes of detonation products are listed in Table 4. According to the order of H_2O–CO–CO_2 in forming detonation products, the detonation products of DNAZ·SA and DNAZ·DNS are calculated as follows:

Table 4. Nitrogen equivalents of different detonation products [28].

Detonation product	H_2O	CO	C	N_2
Nitrogen equivalent index	0.54	0.78	0.15	1

$$C_{10}H_{11}N_3O_7 = (5.5)H_2O + (1.5)CO + (8.5)C + (1.5)N_2$$

$$C_{10}H_9N_5O_{11} = (4.5)H_2O + (6.5)CO + (3.5)C + (2.5)N_2$$

According to Equation (5), in which $M_{DNAZ\cdot SA} = 285.22\ g\,mol^{-1}$, $\rho_{DNAZ\cdot SA} = 1.509\ g\,cm^{-3}$ [5], $M_{DNAZ\cdot DNS} = 375.22\ g\,mol^{-1}$, $\rho_{DNAZ\cdot DNS} = 1.767\ g\,cm^{-3}$ [13], total nitrogen equivalents of DNAZ·SA and DNAZ·DNS are obtained through the nitrogen equivalent indexes of the detonation products in Table 4:

$$\sum N_{DNAZ\cdot SA} = 100 \times (5.5 \times 0.54 + 1.5 \times 0.78 + 8.5 \times 0.15 + 1.5 \times 1)/285.22 = 2.424$$

$$\sum N_{DNAZ\cdot DNS} = 100 \times (4.5 \times 0.54 + 6.5 \times 0.78 + 3.5 \times 0.15 + 2.5 \times 1)/375.22 = 2.805$$

D and *P* can be obtained according to Equations (6) and (7), *D* and *P* of DNAZ·SA are 5916.71 ms^{-1} and 14.04 GPa, respectively, those of DNAZ·DNS are 7684.97 ms^{-1} and 26.25 GPa, respectively. The result conforms to the general rule that the higher oxygen balance leads to the better detonation characterization. The molecular structure analysis for DNAZ·SA and DNAZ·DNS indicates that the nitro group improves the detonation characterization.

4 Conclusions

DSC and TG/DTG methods were used to study the thermal behavior of DNAZ·SA under a non-isothermal condition. Its melting point is 106.15 °C, the T_e and T_p of the intense exothermic decomposition process are 141.18 °C and 153.30 °C, respectively. The E_a and *A* of the intense exothermic decomposition reaction are 92.61 $kJ\,mol^{-1}$ and $10^{9.07}\ s^{-1}$, respectively. The most probable kinetic model functions of the intense exothermic decomposition reaction is Mampel power law $G(\alpha) = \alpha^{1/2}$ and $f(\alpha) = 2\alpha^{1/2}$. The kinetic equation of the intense exothermic decomposition reaction was described as $d\alpha/dT = 2\alpha^{1/2}(10^{9.07}/\beta)\exp(-1.1138 \times 10^4/T)$. The T_{SADT}, T_{p0}, T_{TIT} and T_b are 108.13 °C, 114.20 °C, 120.40 °C, and 129.43 °C, respectively. Above analysis results indicate that DNAZ·DNS has better thermal stability and safety than DNAZ·SA. The results of density functional theory calculations indicate that DNAZ·DNS has better impact insensitivity than DNAZ·SA. The *D* and *P* of DNAZ·SA are 5916.71 ms^{-1} and 14.04 GPa, respectively, those of DNAZ·DNS are 7684.97 ms^{-1} and 26.25 GPa, respectively, which indicate that DNAZ·DNS has better detonation characterization than DNAZ·SA. The results for DNAZ·SA and DNAZ·DNS indicate that the nitro group improves the impact insensitivity, thermal stability, thermal safety and detonation performance. It can be concluded that reasonable layout of nitro group can increase the safety and energy simultaneously.

Acknowledgments

This work was supported by the National Natural Science Foundation of China (Nos. 21673179, 21663033, and 21763030), the China Postdoctoral Science Foundation (No. 2017M613191), the Provincial Natural Science Foundation of Shaanxi (Nos. 2014JQ2068 and 2017JM2039), and the Startup Foundation for Advanced Talents of Yulin University (No. 14GK28).

References

[1] B. S. Tan, M. Huang, J. S. Li, X. P. Long, A new sensitivity criterion of explosives: bonding & nonbonding coupling related molecular rigidity and flexibility (in Chinese), *Chin. J. Energet. Mater.* **2016**, *24*, 10–18.

[2] T. G. Archibald, R.Gilardi, K. Baum, C. George, Synthesis and X-ray crystal structure of 1, 3, 3-trinitroazetidine, *J. Org. Chem.* **1990**, *55*, 2920–2924.

[3] M. A. Hiskey, M. D. Coburn, M. A. Mitchell, B. C. Benicewicz, Synthesis of 3, 3-dinitroazetidine from 1-t-butyl-3,3-dinitroazetidine, *J. Heterocycl. Chem.* **1992**, *29*, 1855–1856.

[4] M. A. Hiskey, M. M. Stincipher, J. E. Brown, Synthesis and initial characterization of some energetic salts of 3,3-dinitroazetidine, *J. Energ. Mater.* **1993**, *11*, 157–165.

[5] R. Gao, B. Yan, T. Mai, Y. Hu, Y. L. Guan, 3,3-Dinitroazetidinium 2-hydroxybenzoate, *Acta Crystallogr. E* **2010**, *66*, o3036.

[6] S. J. Clark, M. D. Segall, C. J. Pickard, P. J. Hasnip, M. J. Probert, K. Refson, M. C. Payne, First principles methods using CASTEP, *Z. Kristallogr.* **2005**, *220*, 567–570.

[7] D. Vanderbilt, Soft self-consistent pseudopotentials in a generalized eigenvalue formalism, *Phys. Rev. B* **1990**, *41*, 7892–7895.

[8] M. C. Payne, M. P. Teter, D. C. Allan, T. A. Arias, J. D. Joannopoulos, Iterative minimization techniques for ab initio total energy calculations: molecular dynamics and conjugate gradients, *Rev. Mod. Phys.* **1992**, *64*, 1045–1097.

[9] B. G. Pfrommer, M. Cote, S. G. Louie, M. L. Cohen, Relaxation of crystals with the quasi-newton method, *J. Comput. Phys.* **1997**, *131*, 233–240.

[10] D. M. Ceperley, B. J. Alder, Ground state of the electron gas by a stochastic method, *Phys. Rev. Lett.* **1980**, *45*, 566–569.

[11] J. P. Perdew, A. Zunger, Self-interaction correction to density-functional approximations for many-electron systems, *Phys. Rev. B* **1981**, 23, 5048–5079.

[12] H. J. Monkhorst, J. D. Pack, Special points for brillouin-zone integrations, *Phys. Rev. B* **1976**, *13*, 5188–5192.

[13] H. X. Ma, B. Yan, Z. N. Li, J. R. Song, R. Z. Hu, Synthesis, molecular structure, non-isothermal decomposition kinetics, and adiabatic time to explosion of 3,3-dinitroazetidinium 3,5-dinitrosalicylate, *J. Therm. Anal. Calorim.* **2009**, *95*, 437–444.

[14] H. X. Ma, B. Yan, Z. N. Li, Y. L. Guan, J. R. Song, K. Z. Xu, R. Z. Hu, Preparation, non-isothermal decomposition kinetics, heat capacity, and adiabatic time-to-explosion of NTO·DNAZ, *J. Hazard. Mater.* **2009**, *169*, 1068–1073.

[15] H. X. Ma, B. Yan, J. F. Li, Y. H. Ren, Y. S. Chen, F. Q. Zhao, J. R. Song, R. Z. Hu, Molecular structure, thermal behavior, and adiabatic time-to-explosion of 3,3-dinitroazetidinium picrate, *J. Mol. Struct.* **2010**, *981*, 103–110.
[16] H. X. Ma, B. Yan, Y. H. Ren, Y. L. Guan, F. Q. Zhao, J. R. Song, R. Z. Hu, Thermal behavior and thermal safety on 3,3-dinitroazetidinium salt of perchloric acid, *J. Therm. Anal. Calorim.* **2011**, *103*, 569–575.
[17] B. Yan, H. X. Ma, N. N. Zhao, T, Mai, J. R. Song, F. Q. Zhao, R. Z. Hu, Thermal behavior, non-isothermal decomposition reaction kinetics and thermal-safety evaluation on N-2,4-dinitrophenyl-3,3-dinitroazetidine under two different pressures, *J. Therm. Anal. Calorim.* **2012**, *110*, 1253–1257.
[18] B. Yan, H. Y. Li, N. N. Zhao, H. X. Ma, J. R. Song, F. Q. Zhao, R. Z. Hu, Thermodynamic properties and detonation characterization of 3,3-dinitroazetidinium hydrochloride, *J. Chem. Eng. Data* **2013**, *58*, 3033–3038.
[19] H. Y. Li, B. Yan, Y. L. Guan, H. X. Ma, J. R. Song, F. Q. Zhao, Thermodynamic properties of 4-amino-3-furazanecarboxamidoxime, *J. Chem. Thermodyn.* **2015**, *90*, 87–91.
[20] B. Yan, H. Y. Li, Y. L. Guan, H. X. Ma, J. R. Song, F. Q. Zhao, Thermodynamic properties of 3,3-dinitroazetidinium nitrate, *J. Chem. Thermodyn.* **2016**, *103*, 206–211.
[21] B. Yan, H. Y. Li, Y. L. Guan, H. X. Ma, J. R. Song, F. Q. Zhao, Thermal behavior and specific heat capacity of 1-t-butyl-3,3-dinitroazetidinium perchlorate, *Propellants Explos. Pyrotech.* **2017**, *42*, 1382–1386.
[22] B. Yan, H. Y. Li, Y. L. Guan, H. X. Ma, J. R. Song, F. Q. Zhao, Thermal behavior and detonation characterization of bis(3,3-dinitroazetidin-1-yl)methane, *Propellants Explos. Pyrotech.* **2018**, *43*, 69–74.
[23] T. L. Zhang, R. Z. Hu, Y. Xie, F. P. Li, The estimation of critical temperatures of thermal explosion for energetic materials using non-isothermal DSC, *Thermochim. Acta* **1994**, 244, 171–176.
[24] R. Z. Hu, S. L. Gao, F. Q. Zhao, Q. Z. Shi, T. L. Zhang, J. J. Zhang, Thermal Analysis Kinetics, second ed., Science Press, Beijing, 2008.
[25] J. H. Yi, F. Q. Zhao, B. Z. Wang, Q. Liu, C. Zhou, R. Z. Hu, Y. H. Ren, S. Y. Xu, K. Z. Xu, X. N. Ren, Thermal behaviors, non-isothermal decompositionreaction kinetics, thermal safety and burning rates of BTATz-CMDB propellant, *J. Hazard. Mater.* **2010**, *181*, 432–439.
[26] W. H. Zhu, H. M. Xiao, First-principles study of electronic, absorption, and thermodynamic properties of crystalline styphnic acid and its metal salts, *J. Phys. Chem. B* **2009**, *113*, 10315–10321.
[27] W. H. Zhu, X. W. Zhang, T. Wei, H. M. Xiao, First-principles study of crystalline mono-amino-2,4,6-trinitrobenzene, 1,3-diamino-2,4,6-trinitrobenzene, and 1,3,5-triamino-2,4,6-trinitrobenzene, *J. Mol. Struct.* (*THEOCHEM*), **2009**, *900*, 84–89.
[28] Y. X. Guo, H. S. Zhang, Nitrogen equivalent and modified nitrogen equivalent equations for predicting detonation parameter of explosives-prediction of detonation velocity of explosives (in Chinese), *Explos. Shock Waves* **1983**, *3*, 56–66.

Manuscript received: July 29, 2018
Revised manuscript received: October 4, 2018
Version of record online: November 15, 2018

